Correlations among angular wave component amplitudes in elastic multiple-scattering random media

Brian G. Hoover,* Louis Deslauriers, Shawn M. Grannell, Rizwan E. Ahmed, David S. Dilworth, Brian D. Athey, and Emmett N. Leith

University of Michigan, Department of Electrical Engineering and Computer Science, Ann Arbor, Michigan 48109-2122

(Received 20 December 2000; revised manuscript received 22 October 2001; published 25 January 2002)

The propagation of scalar waves through random media that provide multiple elastic scattering is considered by derivation of an expression for the angular correlation of the scattered wave amplitudes. Coherent wave transmission is shown to occur through a mechanism similar to that responsible for coherent backscattering. While the properties of the scattered wave are generally consistent with radiative-transfer theory for sufficiently small incident and scattering angles, coherent transmission provides corrections to radiative-transfer results at larger angles. The theoretical angular correlation curves are fit, by specifying the probability densities of two random variables that correspond to material parameters, to measured data of laser light scattering from various polymer microsphere suspensions.

DOI: 10.1103/PhysRevE.65.026614 PACS number(s): 42.25.Dd

I. INTRODUCTION

Wave propagation in multiple-scattering random media is usually treated as an incoherent process. The predominant approach to the analysis of multiple scattering is the theory of radiative transfer [1], which assumes an incoherent process by ignoring interference effects in the scattered wave. This approach is strictly correct only for inelastic scattering processes, such as phonon or Raman scattering. The conventional assumption that a multiplicity of random elastic scattering events completely randomizes the phase of a wave is found to be invalid in situations where the wave can traverse particular scattering paths bidirectionally or identically from more than one direction. These mechanisms lead to effects in elastic multiple-scattering random media that cannot be described as incoherent processes. The mechanism of bidirectional propagation is responsible for strong (Anderson) localization [2] and coherent backscattering (weak localization) [3]. In these effects portions of the wave traverse particular scattering paths in opposite directions and add coherently, which results in intensity enhancements.

Correlations can also be observed between different points on a scattered wave. Under the quasimonochromatic condition of optical coherence theory these correlations are described by the mutual intensity of the wave, $\mathbf{J}(\vec{\mathbf{r}}_1,\vec{\mathbf{r}}_2)$ [4]. Decomposition of an incident wave into its angular (Fourier) spectrum of plane wave components reveals that the mutual intensity of the resulting scattered wave can be expressed as the weighted superposition of the mutual intensities resulting from the scatterings of all possible pairs of Fourier components of the incident wave [5]. A Fourier-component pair forms a harmonically modulated wave with intensity modulation of period Λ. In this paper we present a scalar wave model that describes correlations among Fourier components of waves (angular correlation) in elastic multiple-scattering random media when the period Λ is much larger than the size of the scattering structures. The theory is compared with data from laser light scattering experiments.

A familiar result of our analysis is the angular memory effect, which was initially predicted for light wave propagation in elastic multiple-scattering random media by Feng and coworkers [6,7], although it had been recognized earlier in laser light reflected by single-scattering random surfaces [8] and even earlier in light propagation through volume turbulence [9]. The angular correlation of optical wave amplitudes reflected from one-dimensional surface roughness distributions that provide multiple elastic scattering has been studied by simulation [10] and theoretical and experimental angular correlation results have been reported for laser light transmission through random phase screens [11]. Recently the role of plasmon polaritons in the angular correlation of light scattered from weakly rough metallic surfaces has been established [12]. The scattering theory presented in this paper unifies many of the earlier results through a complete analytical description of the mutual intensity of multiply scattered scalar waves in elastic media. We point out that while previous scattering models [6,7] accurately predict the memory effect in multiple elastic scattering, they provide an incomplete description of the mutual intensity of the scattered field.

II. ANGULAR CORRELATION AND MUTUAL INTENSITY OF SCATTERED FIELD

The physical setting of interest is depicted in Fig. 1. Two plane waves of equal amplitude specified by the wave-vectors $\vec{\mathbf{k}}_{i1}$ and $\vec{\mathbf{k}}_{i2}$ that lie in the xz plane are incident on the scattering medium. The incident wave vectors are given by $\vec{\mathbf{k}}_i = 2\pi(\hat{x}\sin\theta_i + \hat{z}\cos\theta_i)/\lambda$. The medium is in the form of a slab of surface area s^2, and $s \gg l$ where l is the scattering mean free path. Figure 1(a) details an initial scattering event occurring at a depth z_a from the front of the slab. With $\theta_{i1} = -\theta_{i2}$ for illustration, the total field incident on the

*Present address: Applied Technology Associates, 1900 Randolph Rd. SE, Albuquerque, NM 87106.
Email address: Hoover@engin.umich.edu

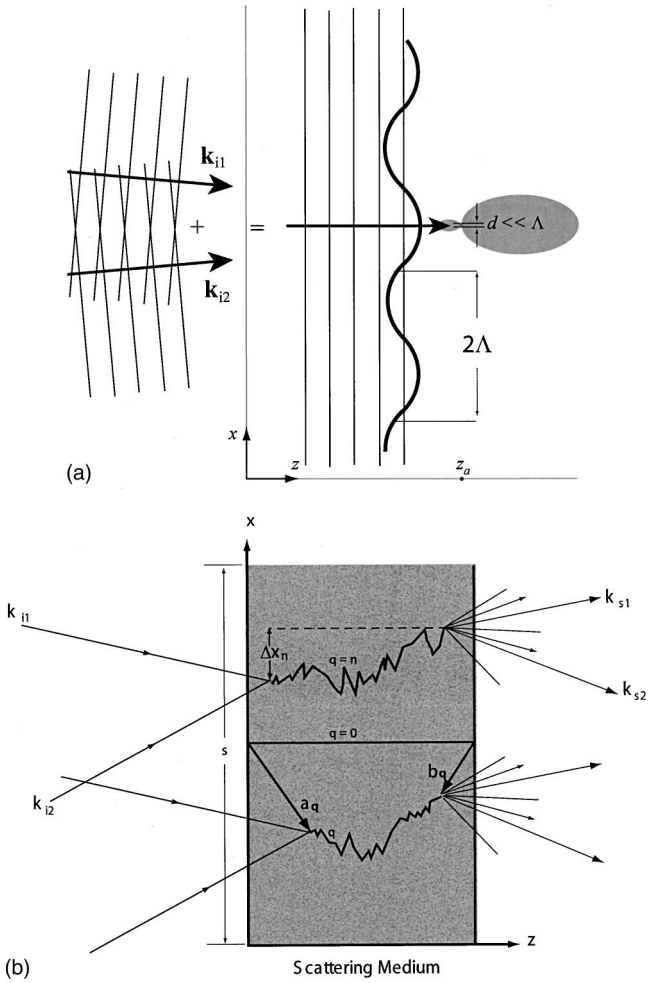

FIG. 1. (a) Schematic representation of a pair of plane waves incident on a scattering structure near the front surface of a random medium. The structure linear dimension d is much smaller than the period Λ of the interference pattern formed by the plane waves. (b) Schematic of the paired trajectory model depicting two representative trajectories and the random variables Δx, $\vec{\mathbf{a}}$, and $\vec{\mathbf{b}}$ that determine the coherent transmission properties.

scattering structure is $\exp(jkx\sin\theta_{i1})+\exp[-jkx\sin\theta_{i1}]=2\cos(kx\sin\theta_{i1})$, which describes a normally incident plane wave with amplitude modulation of period $2\Lambda=\lambda/\sin\theta_{i1}$. If the maximum linear dimension of the scattering structure is $d\ll\Lambda$ then the initial scattering is essentially that of a plane wave of intensity $4\cos^2(kx_a\sin\theta_{i1})$, where (x_a,z_a) are the coordinates of the scatterer. Importantly, under the condition $d\ll\Lambda$ it is impossible to distinguish the contributions of the waves specified by $\vec{\mathbf{k}}_{i1}$ and $\vec{\mathbf{k}}_{i2}$ to the angular scattering profile. This assumption has been used previously, for instance, in the fringe model of cross-beam laser velocimetry [13]. It implies that the scattering trajectories indicated in Fig. 1(b) are traversed identically from the two directions specified by $\vec{\mathbf{k}}_{i1}$ and $\vec{\mathbf{k}}_{i2}$. This hypothesis enables derivation of the mutual intensity of the scattered field in terms of the scattering parameters of the slab.

The coherence of the scattered field can be described by the mutual intensity $\mathbf{J}(\vec{\mathbf{r}}_1,\vec{\mathbf{r}}_2)$ on the exit surface of the slab, or equivalently by the Fourier mutual intensity $\mathcal{J}(\vec{\mathbf{k}}_{s1},\vec{\mathbf{k}}_{s2})$, where $\vec{\mathbf{k}}_s$ is the scattered wave vector. When the incident wave consists only of the pair of correlated unit-amplitude plane waves specified by $\vec{\mathbf{k}}_{i1}$ and $\vec{\mathbf{k}}_{i2}$, the Fourier mutual intensity becomes a characteristic of the scattering medium and is denoted by $\mathcal{J}(\vec{\mathbf{k}}_{s1},\vec{\mathbf{k}}_{s2};\vec{\mathbf{k}}_{i1},\vec{\mathbf{k}}_{i2})$, which is known as the field or amplitude angular correlation. Together with the angular intensity distribution $\mathcal{I}(\vec{\mathbf{k}}_s,\vec{\mathbf{k}}_i)$ the field angular correlation determines the mutual intensity on the exit surface through the relation

$$\mathbf{J}(\vec{\mathbf{r}}_1,\vec{\mathbf{r}}_2)=2\int[\mathcal{I}(\vec{\mathbf{k}}_s;\vec{\mathbf{k}}_{i1})+\mathcal{I}(\vec{\mathbf{k}}_s;\vec{\mathbf{k}}_{i2})]\times\exp[j\vec{\mathbf{k}}_s\cdot(\vec{\mathbf{r}}_1-\vec{\mathbf{r}}_2)]d\vec{\mathbf{k}}_s+4\cos[\Delta\vec{\mathbf{k}}_i\cdot(\vec{\mathbf{r}}_1+\vec{\mathbf{r}}_2)]\times\int\mathcal{J}(\Delta\vec{\mathbf{k}}_i,\overline{\mathbf{k}}_i,\overline{\mathbf{k}}_s)\exp[j\overline{\mathbf{k}}_s\cdot(\vec{\mathbf{r}}_1-\vec{\mathbf{r}}_2)]d\overline{\mathbf{k}}_s,\quad(1)$$

where $2\Delta\overline{\mathbf{k}}_i$ is the difference of the incident wave vectors and $\overline{\mathbf{k}}_{i,s}$ is the mean incident or scattered wave vector. Equation (1) is derived by starting with the fundamental relation between $\mathbf{J}(\vec{\mathbf{r}}_1,\vec{\mathbf{r}}_2)$ and $\mathcal{J}(\vec{\mathbf{k}}_{s1},\vec{\mathbf{k}}_{s2})$ [5], expressing $\mathcal{J}(\vec{\mathbf{k}}_{s1},\vec{\mathbf{k}}_{s2})$ in terms of $\mathcal{J}(\vec{\mathbf{k}}_{s1},\vec{\mathbf{k}}_{s2};\vec{\mathbf{k}}_{i1},\vec{\mathbf{k}}_{i2})$ [5], and changing to sum and difference wave vector variables and applying the angular memory effect, which is derived as part of the following analysis. Note that Eq. (1) is the sum of the Fourier transforms of the angular intensity and the angular correlation. On the exit surface the pair of scattered plane waves generates a fringe pattern given by

$$I(\vec{\mathbf{r}})=\mathbf{J}(\vec{\mathbf{r}},\vec{\mathbf{r}})=2\int[\mathcal{I}(\vec{\mathbf{k}}_s;\vec{\mathbf{k}}_{i1})+\mathcal{I}(\vec{\mathbf{k}}_s;\vec{\mathbf{k}}_{i2})]d\vec{\mathbf{k}}_s+4\cos[2\Delta\vec{\mathbf{k}}_i\cdot\vec{\mathbf{r}}]\int\mathcal{J}(\Delta\vec{\mathbf{k}}_i,\overline{\mathbf{k}}_i,\overline{\mathbf{k}}_s)d\overline{\mathbf{k}}_s.\quad(2)$$

The fringe contrast is, therefore, determined by the integral of the angular correlation over the mean scattered wavevector $\overline{\mathbf{k}}_s$.

Equation (1) should be compared with the coherence function derived from radiative-transfer theory [14]

$$\mathbf{J}_{\mathrm{RT}}(\vec{\mathbf{r}}_1,\vec{\mathbf{r}}_2)\simeq\int\mathcal{I}(\overline{\mathbf{r}},\vec{\mathbf{k}}_s)\exp[j\vec{\mathbf{k}}_s\cdot(\vec{\mathbf{r}}_1-\vec{\mathbf{r}}_2)]d\vec{\mathbf{k}}_s,\quad(3)$$

where $\mathcal{I}(\overline{\mathbf{r}},\vec{\mathbf{k}}_s)$ is the angular intensity emanating from coordinate $\overline{\mathbf{r}}\equiv(\vec{\mathbf{r}}_1+\vec{\mathbf{r}}_2)/2$. Equation (3) is valid only for fields that exhibit negligible intensity variations over their coherence area, which are also known as a quasihomogeneous fields. Equation (3) can be clearly revealed as incorrect when applied to fields that exhibit harmonic intensity variation [15], however, Eq. (1) is valid for all harmonic-intensity fields and can be extended to describe fields of arbitrary intensity.

III. MULTIPLE-SCATTERING MODEL OF ANGULAR CORRELATION

For derivation of an expression for the field angular correlation of the scattering slab we refer to Fig. 1(b). For each realization p of the random process that describes the scattering medium there are N scattering trajectories, which are labeled with the index $q=1,2,\ldots,n,\ldots,N$. $q=0$ denotes a phantom reference trajectory that lies along a perpendicular line from the front to the back surface, relative to which the phase delays of the actual trajectories are expressed. The convention is adopted that the trajectory $q=1$ is that trajectory with scattering centers at the smallest cumulative distance from the trajectory $q=0$, with the scattering centers of $q=2$ being the next closest and so on. With $P_{pq}\geqslant 0$ denoting the pencil-beam amplitude-spread function, the total field scattered with wave vector $\vec{\mathbf{k}}_s$ that derives from the incident wave vector $\vec{\mathbf{k}}_i$ is

$$\mathbf{E}_p(\vec{\mathbf{k}}_s;\vec{\mathbf{k}}_i)=\sum_{q=1}^{N} P_{pq}\exp[j\varphi_{pq}(\vec{\mathbf{k}}_i,\vec{\mathbf{k}}_s)] \tag{4}$$

for the pth realization of the ensemble. $\varphi_{pq}(\vec{\mathbf{k}}_i,\vec{\mathbf{k}}_s)$ is the phase delay relative to the reference of the wave traversing the qth trajectory and consists of three parts: the phase delay $\varphi_{pqa}(\vec{\mathbf{k}}_i)$ incurred due to the separation of the initial points of the trajectories $q=0$ and q, the phase delay φ_{pqv} due to the different path lengths of the trajectories $q=0$ and q, and the phase delay $\varphi_{pqb}(\vec{\mathbf{k}}_s)$ due to the separation of the terminal points of the two trajectories. Therefore, Eq. (4) may be written as

$$\mathbf{E}_p(\vec{\mathbf{k}}_s,\vec{\mathbf{k}}_i)=\sum_{q=1}^{N} P_{pq}\exp\{j[\varphi_{pqa}(\vec{\mathbf{k}}_i)+\varphi_{pqv}+\varphi_{pqb}(\vec{\mathbf{k}}_s)]\}. \tag{5}$$

The field angular correlation is then calculable as

$$\mathcal{T}(\vec{\mathbf{k}}_{s1},\vec{\mathbf{k}}_{s2};\vec{\mathbf{k}}_{i1},\vec{\mathbf{k}}_{i2})=\langle \mathbf{E}_p(\vec{\mathbf{k}}_{s1};\vec{\mathbf{k}}_{i1})\mathbf{E}_p^*(\vec{\mathbf{k}}_{s2},\vec{\mathbf{k}}_{i2})\rangle, \tag{6}$$

where $\langle\cdots\rangle$ denotes the ensemble average. Inserting Eq. (5) into Eq. (6) and changing the order of operations leads to

$$\begin{aligned}\mathcal{T}(\vec{\mathbf{k}}_{s1},\vec{\mathbf{k}}_{s2};\vec{\mathbf{k}}_{i1},\vec{\mathbf{k}}_{i2})=\sum_{q=1}^{N}\sum_{r=1}^{N}\langle P_{pq}P_{pr}\exp\{j[&\varphi_{pqa}(\vec{\mathbf{k}}_{i1})\\&+\varphi_{pqv}+\varphi_{pqb}(\vec{\mathbf{k}}_{s1})-\varphi_{pra}(\vec{\mathbf{k}}_{i2})-\varphi_{prv}\\&-\varphi_{prb}(\vec{\mathbf{k}}_{s2})]\}\rangle.\end{aligned} \tag{7}$$

With the possible exception of terms with the smallest values of q and r, all terms for which $q\neq r$ in the summation of Eq. (7) are negligible, because the phase difference between two trajectories will vary by more than 2π over the ensemble unless both differ from the reference trajectory by less than a wavelength. If all of the scattering centers on certain trajectories are at distances from the reference much less than a wavelength, then the corresponding terms in Eq. (7) may not average to zero. Such trajectories correspond to ballistic wave transmission. Hence all terms for which $q\neq r$ in the summation of Eq. (7) are negligible if we restrict attention to nonballistic transmission. For $q=r$ the phase contribution due to the path length difference between trajectories vanishes, leaving

$$\begin{aligned}\mathcal{T}(\vec{\mathbf{k}}_{s1},\vec{\mathbf{k}}_{s2};\vec{\mathbf{k}}_{i1},\vec{\mathbf{k}}_{i2})&=\sum_{q=1}^{N}\langle P_q^2\exp\{j[\varphi_{qa}(\vec{\mathbf{k}}_{i1})+\varphi_{qb}(\vec{\mathbf{k}}_{s1})\\&\quad-\varphi_{qa}(\vec{\mathbf{k}}_{i2})-\varphi_{qb}(\vec{\mathbf{k}}_{s2})]\}\rangle\\&=\left\langle\sum_{q=1}^{N}P_q^2\exp[j\Phi_q(\vec{\mathbf{k}}_{i1},\vec{\mathbf{k}}_{i2},\vec{\mathbf{k}}_{s1},\vec{\mathbf{k}}_{s2})]\right\rangle,\end{aligned} \tag{8}$$

with the index p hereafter made implicit. It will be shown that the phase function $\Phi_q(\vec{\mathbf{k}}_{i1},\vec{\mathbf{k}}_{i2},\vec{\mathbf{k}}_{s1},\vec{\mathbf{k}}_{s2})$ can in fact vary by less than 2π over the ensemble, which provides for angular correlation and coherent wave transmission according to Eq. (1)

In order to express the phase function Φ_q in terms of the parameters of the scattering slab we introduce the vectors $\vec{\mathbf{a}}_q=(x_{qa},y_{qa},z_{qa})$ and $\vec{\mathbf{b}}_q=(x_{qb},y_{qb},z_{qb})$, which, as drawn in Fig. 1(b), point from the initial and terminal points of the reference trajectory, respectively, to the initial and terminal scattering centers of the qth trajectory, respectively. By simple geometry the phase delays are then

$$\varphi_{qa}(\vec{\mathbf{k}}_i)=\vec{\mathbf{k}}_i\cdot\vec{\mathbf{a}}_q, \tag{9}$$

$$\varphi_{qb}(\vec{\mathbf{k}}_s)=-\vec{\mathbf{k}}_s\cdot\vec{\mathbf{b}}_q. \tag{10}$$

From Eqs. (8)–(10)

$$\Phi_q(\vec{\mathbf{k}}_{i1},\vec{\mathbf{k}}_{i2},\vec{\mathbf{k}}_{s1},\vec{\mathbf{k}}_{s2})=(\vec{\mathbf{k}}_{i1}-\vec{\mathbf{k}}_{i2})\cdot\vec{\mathbf{a}}_q+(\vec{\mathbf{k}}_{s2}-\vec{\mathbf{k}}_{s1})\cdot\vec{\mathbf{b}}_q. \tag{11}$$

Choosing scattered wavevectors in the xz plane and introducing the variable

$$\Delta x_q=x_{qb}-x_{qa}, \tag{12}$$

Eq. (11) can be expanded as

$$\begin{aligned}\Phi_q(\vec{\mathbf{k}}_{i1},\vec{\mathbf{k}}_{i2},\vec{\mathbf{k}}_{s1},\vec{\mathbf{k}}_{s2})&=\frac{2\pi}{\lambda}[(\sin\theta_{i1}-\sin\theta_{i2}+\sin\theta_{s2}-\sin\theta_{s1})\\&\quad\times x_{qa}+(\sin\theta_{s2}-\sin\theta_{s1})\Delta x_q\\&\quad+(\cos\theta_{i1}-\cos\theta_{i2})z_{qa}+(\cos\theta_{s2}-\cos\theta_{s1})z_{qb}].\end{aligned} \tag{13}$$

The ensemble variation of each term within the square brackets must be limited to less than λ for correlation to exist. Two forms of correlation can occur, which differ in the ranges of the trajectory index q that contribute to the effect.

1. Local correlation. If the differences between both the incident and the scattered wave vectors are sufficiently small,

then local correlation may arise within subsets of the paired trajectories, that is, within subsets of the index q. There are various combinations of conditions that can lead to this form of correlation. As an illustrative example consider a single incident plane wave, i.e., $\vec{\mathbf{k}}_{i1}=\vec{\mathbf{k}}_{i2}$. Equation (13) then becomes

$$\Phi_q(\vec{\mathbf{k}}_i,\vec{\mathbf{k}}_i,\vec{\mathbf{k}}_{s1},\vec{\mathbf{k}}_{s2})=\frac{2\pi}{\lambda}[(\sin\theta_{s2}-\sin\theta_{s1})x_{qb}+(\cos\theta_{s2}-\cos\theta_{s1})z_{qb}]. \quad (14)$$

Again the bracketed quantity must vary by less than λ for correlation to exist. This cannot occur for arbitrarily large values of q because $\max(x_q)\gg\lambda$ for large q, however due to the angular coefficients the random variables x_{qb} and z_{qb} can range over distances larger than λ, which implies that coherence on the exit surface can occur through this mechanism without the presence of a ballistic wave. This effect is related to the so-called snake light of optical wave transmission [16]. Note that the ranges of x_{qa} and z_{qa} will also be restricted due to the convention for indexing the trajectories. Local correlation arises around any reference trajectory realized by translation of the original reference in the (x,y) plane and, therefore, the local correlation produces a mutual intensity that is shift invariant. The scattered fields at points separated by distances larger than the local correlation width remain uncorrelated under this effect, and the addition of uncorrelated waves from different volumes produces an incoherent field in the angular domain or zero angular correlation. The local correlation, therefore, generates on the exit surface a quasihomogeneous field as described by the generalized Van Cittert-Zernike theorem of optical coherence theory [4].

2. Angular correlation. Equation (8) indicates that angular correlation can exist only if the ensemble average over all of the paired trajectories is nonzero, because the summation in Eq. (8) may be interpreted as an average over q. This requirement is consistent with the fact that points in the angular domain receive wave contributions from every trajectory. In order to realize this effect the first term in the square brackets of Eq. (13) must be eliminated, because if all values of q are to be included then $\max(x_q)=s\gg\lambda$. This implies that the condition

$$\vec{\mathbf{k}}_{i1}-\vec{\mathbf{k}}_{i2}=\vec{\mathbf{k}}_{s1}-\vec{\mathbf{k}}_{s2} \quad (15)$$

is necessary for angular correlation. The condition of Eq. (15) is the angular memory effect. Assuming this condition and including the average over q Eq. (13) becomes

$$\Phi(\vec{\mathbf{k}}_{i1},\vec{\mathbf{k}}_{i2},\vec{\mathbf{k}}_{s1},\vec{\mathbf{k}}_{s2})=2\pi\left[\frac{\Delta x}{\Lambda}+(\cos\theta_{i1}-\cos\theta_{i2})\frac{z_a}{\lambda}+(\cos\theta_{s2}-\cos\theta_{s1})\frac{z_b}{\lambda}\right], \quad (16)$$

where $\Lambda=\lambda/(\sin\theta_{i2}-\sin\theta_{i1})$ is the intensity fringe period. Again due to the memory effect it can be shown that

$$\cos\theta_{s2}-\cos\theta_{s1}=-\frac{\lambda}{\Lambda}\tan\overline{\theta_s} \quad (17)$$

for sufficiently small $(\theta_{s2}-\theta_{s1})$, where $\overline{\theta_s}=(\theta_{s2}+\theta_{s1})/2$ is the mean scattering angle. Substituting Eq. (17) into Eq. 16 and assuming that the incident wave vectors are symmetrically oriented about the normal to the front surface of the slab reduces Eq. (16) to the simple expression

$$\Phi(\vec{\mathbf{k}}_{i1},\vec{\mathbf{k}}_{i2},\vec{\mathbf{k}}_{s1},\vec{\mathbf{k}}_{s2})=K(\Delta x-z_b\tan\overline{\theta_s}), \quad (18)$$

with $K\equiv 2\pi/\Lambda$. The function of Eq. (18) must vary by less than 2π over the ensemble for angular correlation to exist. In contrast to local correlation [Eq. (14)] for which the scattering parameters must vary by less than the wavelength λ, Eq. (18) implies that angular correlation occurs for scattering and associated material parameters that vary by less than the spatial fringe period Λ. Note from Eq. (18) that at zero mean scattering angle the angular correlation phase is determined exclusively by the range of the migration variable Δx. Since Δx can, in principle, be described by a radiative-transfer model this implies that radiative transfer is strictly correct only for small mean (incident and scattered) angles, and that the term in z in Eq. (18) serves as a correction to radiative transfer results due to coherent effects at larger angles.

It is useful to recognize the correspondences of the local and angular correlations to the mutual intensity terms given in Eq. (1). The local correlation generates a quasihomogeneous field that contributes to the mutual intensity on the exit surface but not in the angular domain; referring to Eq. (1) it must then correspond to the Fourier transform of the angular intensity $[\mathcal{I}(\vec{\mathbf{k}}_s;\vec{\mathbf{k}}_{i1})+\mathcal{I}(\vec{\mathbf{k}}_s;\vec{\mathbf{k}}_{i2})]$, which implies that the local correlation exclusively determines the angular intensity distribution. While the contribution of the angular correlation to the mutual intensity on the surface is not obvious from the preceding scattering analysis, the angular correlation obviously corresponds to the transform of $\mathcal{J}(\Delta\vec{\mathbf{k}}_i,\overline{\mathbf{k}_i},\overline{\mathbf{k}_s})$ in Eq. (1). Angular correlation, therefore, generally contributes to the coherence both on the surface and in the angular domain, which implies that the scattered field is generally nonquasihomogeneous under this effect.

Use of the continuum approximation in previous derivations of the memory effect [6,7] serves to omit the term in z in Eq. (18) and leads to what is essentially a radiative-transfer result. Omission of the term in z in Eq. (18) leads to an angular correlation that is independent of the mean scattered angle $\overline{\mathbf{k}_s}$ and neglects the second integral of Eq. (1), leading to a generally incomplete description of the mutual intensity of the scattered field.

Interpretation of Eq. (18) provides a classification of elastic multiple-scattering processes by phasor diagrams as illustrated in Fig. 2. The diagrams schematically depict the ranges of the random functions of Eq. (18) for large values of $\overline{\theta_s}$ in representative cases of large and small deviations σ_z. σ_z corresponds to the scattering mean free path in volume media or to the surface variance in surface scattering. Coherent effects occur if the phasor diagram closes within the range of the random function in z, in which case the second

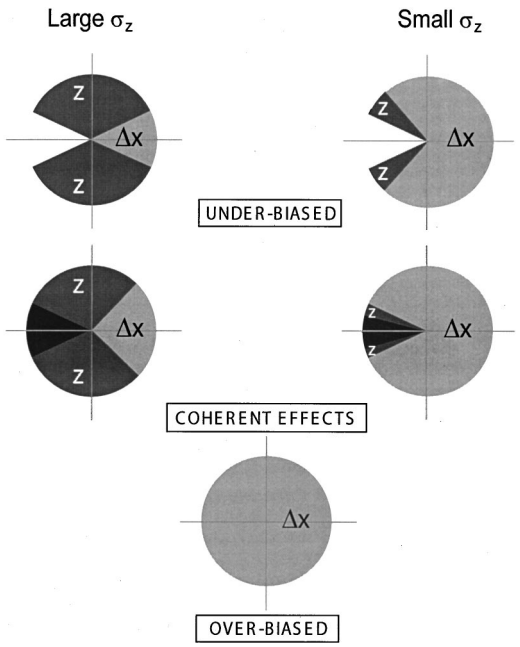

FIG. 2. Phasor diagrams that schematically classify elastic multiple-scattering processes according to the coherence on the exit surface of the medium.

term in Eq. (1) contributes to the mutual intensity on the surface. The migration variable Δx may be interpreted as a bias for the presence of coherent effects. Recalling Eq. (2), in this terminology the underbiased process exhibits high-contrast interference fringes at all scattering angles $\overline{\theta_s}$, the coherent process exhibits fringes only over a lower range of $\overline{\theta_s}$, while the interference fringes are washed out at all angles in the overbiased process.

IV. OPTICAL MEASUREMENT SYSTEM

We have measured the angular intensity and the modulus of the angular correlation as functions of scattering angle for laser light transmission through various suspensions of polymer microspheres. The experimental configuration is shown in Fig. 3. A helium-neon laser beam ($\lambda = 633$ nm) is split in a Mach-Zehnder interferometer and expanded in a Keplerian telescope to form a horizontal pattern of interference fringes with $\Lambda = 1.25$ mm ($\theta_{i1} = 0$, $\theta_{i2} = 0.029°$) over a beam diameter of 15 cm, which is incident on the microsphere suspension held in a $(90 \times 45 \times 3.75)$-mm^3 glass tank. An electronic shutter is used to ensure that the laser energy incident on the tank per camera exposure is constant.

The modulus of the angular correlation is proportional to the fringe contrast in the scattered light, which is measured over a large mean scattering angle ($\overline{\theta_s}$) range by mounting an imaging system on a rotary rail, which includes a spatial filter to define a scattering angle bin size (1.15° here) over which $|\mathcal{J}(\Delta\vec{\mathbf{k}}_i, \overline{\mathbf{k}_i}, \overline{\mathbf{k}_s})|$ is averaged, a Glan-Thompson polarizer to eliminate vector-wave scattering effects, and a *TE* cooled 12-bit charge coupled device (CCD) array with variable exposure time. The angular intensity distribution is obtained by adding the intensities arising from sequential illumination with the waves from the two interferometer arms. Ballistic wave transmission is excluded by a slight vertical shift of the spatial filter bandpass. Measurements were taken through 30° with this configuration for aqueous suspensions of 2-μm diameter acrylic latex spheres and 10-μm diameter polystyrene-divinylbenzene (PS-DVB) spheres. The relative concentrations of the polymer suspensions were measured volumetrically.

Fringe contrast as a function of angle $\overline{\theta_s}$ is determined as the classical visibility

$$\mathcal{V} = \frac{I_{\max} - I_{\min}}{I_{\max} + I_{\min}} \tag{19}$$

over the single fringe period that coincides with the axis of rotation of the imaging rail. The recorded fringe visibility decreases away from the rotary axis due to defocus. The fidelity of the measurement system is verified with an incoherent fringe pattern produced by collimated laser-beam incidence on a bar-pattern transparency affixed to a glass plate coated with white spray paint. The number of CCD pixels per fringe period in the image is greater than 20 to avoid contrast reduction by the modulation transfer function of the camera. The microsphere suspensions are kept agitated by stirring and the camera exposure times are sufficiently long to wipe out speckle noise and approximate ensemble averages.

V. COMPARISON WITH EXPERIMENTAL DATA

Figure 4 presents representative data acquired with the system of Fig. 3. The normalized angular intensity distribution (solid line) and the angular correlation (dashed line) of a

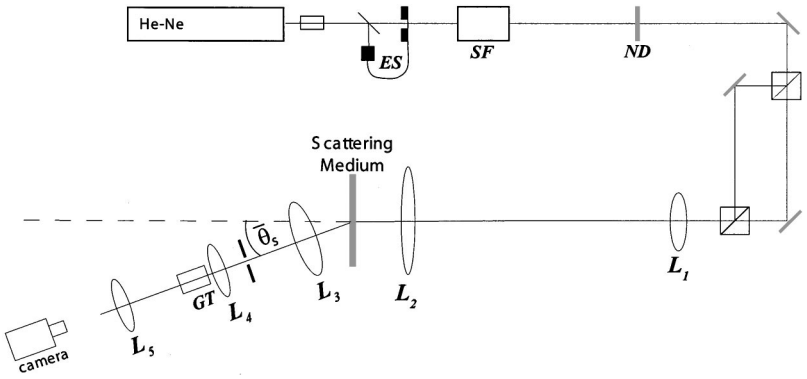

FIG. 3. Optical system for angular correlation measurements. ES electronic shutter; SF, spatial filter; ND, neutral density filter, L_1, 35 mm lens; L_2, 1500 mm lens, L_3, 100 mm $f/2.3$ lens; L_4, 50 mm $f/2$ lens; GT, Glan-Thompson polarizer, L_5, 50 mm $f/1.8$ lens.

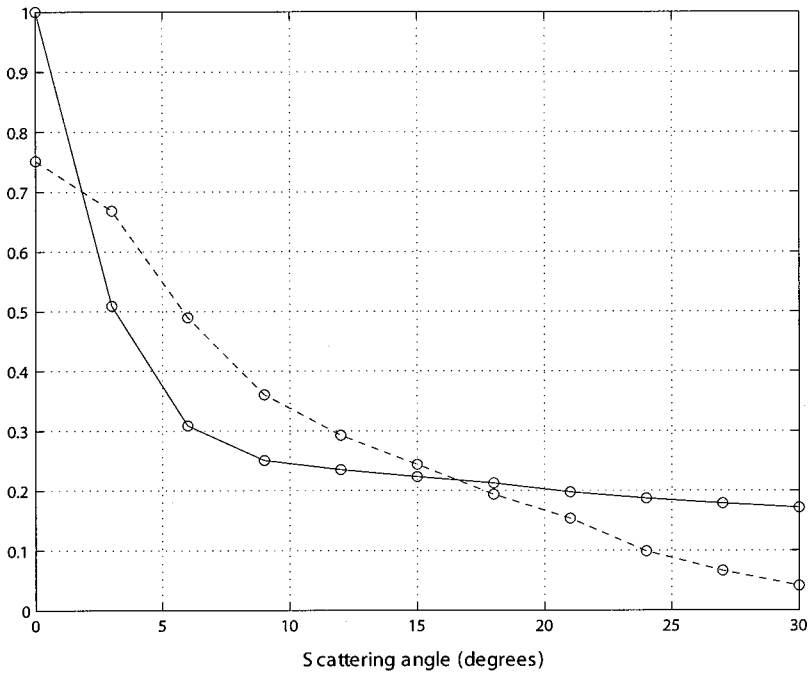

FIG. 4. Angular intensity (solid) and field angular correlation (dashed) data of laser light scattered by a suspension of 10-μm diameter polymer spheres. The incident wave vectors make angles of 0° and 0.029° to the plane of the medium ($\Lambda = 1.25$ mm).

suspension of 10-μm-diameter PS-DVB spheres are shown. The horizontal axis in Fig. 4 is the external scattering angle or the external mean scattering angle for the intensity and angular correlation curves, respectively. These curves determine the mutual intensity at the surface of the suspension according to Eq. (1).

The angular correlation data must be compared with the predictions of the scattering model. Model angular correlation curves are produced by substituting from Eq. (18) into Eq. (8) with appropriate statistical models of the random variables Δx and z_b. z_b is assumed to be power-law distributed in the form

$$\rho_z(z) = N \,\mathrm{rect}\left(\frac{z + L/2}{L}\right)(1-f)^{-z/d\cos\overline{\theta}_s}, \tag{20}$$

where f is the volume fraction or the probability of a scattering particle occupying any infinitesimal volume, d is the particle diameter, and $N = -\ln(1-f)/d\cos\overline{\theta}_s$. The distribution ρ_z is maximum at $z_b = 0$, which corresponds to terminal scattering at the exit surface, and is truncated at $z_b = -L$, where L is the slab thickness, which is assumed to be much greater than the particle diameter d. The distribution of Δx is not as simply derived. $\rho_{\Delta x}$ is essentially the average intensity distribution due to transmission of a pencil beam through the slab, however, there exists no generally proven and expressible radiative-transfer solution for transmission of a narrow beam through anisotropically scattering particles. It has been demonstrated that neither the diffusion nor the first-order multiple-scattering approximation to the radiative-transfer equation can accurately describe scattering suspensions as those used for our measurements [17]. Fortunately, as will be shown directly, the influence of $\rho_{\Delta x}$ on the angular correlation curve at a particular wave number K is simply a multiplicative constant. Therefore, the scattering model can be compared to data at a particular K without knowledge of $\rho_{\Delta x}$ through incorporation of a multiplicative data-fitting parameter.

Substituting from (18) into Eq. (8) and noting that $P^2 = \rho_{\Delta x}$ leads to the angular correlation expression

$$\mathcal{J}(\Delta\vec{\mathbf{k}}_i, \overline{\mathbf{k}}_s) = \int\int \exp[jK(\Delta x - z\tan\overline{\theta}_s)] \times \rho^2_{\Delta x}(\Delta x)\rho_z(z)d\Delta x\, dz, \tag{21}$$

where Δx and z are assumed to be independently distributed. In Eq. (21) the wave vector variable $\Delta\vec{\mathbf{k}}_i$ determines K, $\overline{\mathbf{k}}_s$ determines $\overline{\theta}_s$, and $\overline{\mathbf{k}}_i = \mathbf{0}$. Consistent with previous derivations of the memory effect [7] the integral over Δx can be expressed as the Fourier transform of $\rho^2_{\Delta x}$, which leads to the expression

$$\mathcal{J}(\Delta\vec{\mathbf{k}}_i, \overline{\mathbf{k}}_s) = A(K)\int \rho_z(z)\exp[-jKz\tan\overline{\theta}_s]dz. \tag{22}$$

The form of $A(K)$ in the diffusion approximation is given in the previous work [7]. The integral in Eq. (22) can be evaluated symbolically as

$$\mathcal{J}(\Delta\vec{\mathbf{k}}_i, \overline{\mathbf{k}}_s) = A(K)\frac{\ln(1-f)[\ln(1-f) + jKd\sin\overline{\theta}_s]}{[\ln^2(1-f) + K^2d^2\sin^2\overline{\theta}_s]}. \tag{23}$$

Thus the scattering model predicts a complex angular correlation with Hermitian symmetry as a function of $\overline{\theta}_s$. Complex angular correlation has been observed in simulations of light scattering from metallic surfaces [10], while measurements with polymer microspheres have revealed Hermitian symmetry [5].

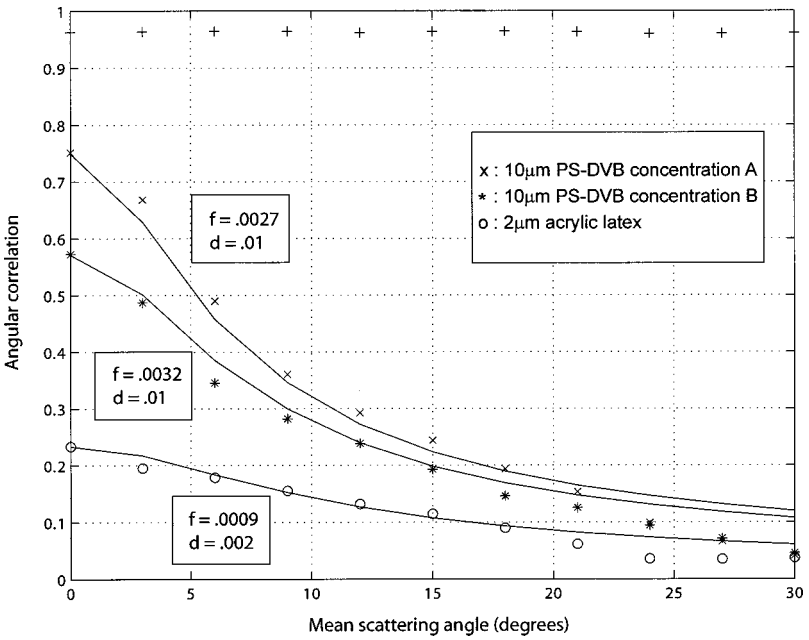

FIG. 5. Field angular correlation vs mean scattering angle $\overline{\theta_s}$ for transmission through several microsphere suspensions. The incident wave vectors are fixed such that $\Lambda = 1.25$ mm. The parameters f and d used to generate the solid model curves are given for each suspension. The relative concentrations of the PS-DVB suspensions were measured as $[A]/[B] \approx 0.8$. The data along the top of the plot (+) is obtained for an incoherent fringe pattern of the same period.

The modulus of the angular correlation given in Eq. (23) is fit to the experimental data as shown in Fig. 5. The values of K and d are known and $A(K)$ is chosen to match the data at $\overline{\theta_s} = 0$. The remaining parameter of volume fraction f used to generate the solid model curves is indicated adjacent to each curve. Deviations from the data at angles greater than 20° are possibly due to the correlation of the variables Δx and z at larger angles. Somewhat better fits to the PS-DVB data are achieved with volume fraction values in ratios closer to unity than the concentration measurements would corroborate. The smaller volume fraction of the acrylic latex suspension follows from the smaller particle diameter and the wider angular scattering profile of the single particle according to the Mie theory. The data points along the top of the plot indicate the angular correlation response of the system to an incoherent input with $\Lambda = 1.25$ mm.

VI. CONCLUSIONS

We have described a model for the angular correlation of wave fields applicable to elastic multiple-scattering media, which is based on a paired-trajectory mechanism similar to that responsible for coherent backscattering. The model also accounts for the well-known local field correlation. These correlations have been related to the spatial coherence in the medium as given by the mutual intensity function. In addition to rederiving the well-known memory effect the angular correlation model makes several predictions. Angular correlation is predicted to occur for random trajectories that vary by less than the spatial fringe period Λ rather than the wavelength λ as in the case of local correlation. The presence of angular correlation is also found to generally imply a nonquasihomogeneous field. An angular correlation phase function is considered, which consists of a bias term consistent with radiative-transfer theory and terms that increase with the incident and scattered angles and appear as corrections to radiative-transfer results. The model angular correlation is complex with Hermitian symmetry in the mean scattering angle. While the scattering theory is presented in the context of scalar optical wavefields it is equally applicable to any scalar wave field propagating in an elastic multiple-scattering medium.

Several applications of the theory could arise through further research. Expanded statistical modeling of the random variables used to express the angular correlation phase function in Eq. (18) could provide powerful new techniques for material characterization based on coherence measurements. Characterization efforts should be aided by the separability of the angular correlation into functions of $\Delta\vec{\mathbf{k}}_i$ (or K) and $\overline{\mathbf{k}}_s$ (or $\overline{\theta_s}$) evident in Eq. (23). In particular according to Eq. (23) the angular correlation variation with $\overline{\theta_s}$ is independent of the sample thickness L when $L \gg d$. If the material parameters are known, the theory provides an analytical form for the angular correlation that is applicable to coherent wave transport and imaging into or through elastically scattering media. Detection techniques based on angular correlation have already been reported in the radar field [18,19].

ACKNOWLEDGMENTS

The authors would like to thank Jim Trolinger, Stephen Rand, and Ted Norris for useful suggestions. Kurt Mills provided laboratory support, and Zeev Zalevsky reviewed the draft manuscript. This research was supported by the National Institutes of Health under NLM Contract No. N01-LM-0-3511 and NCI Contract No. N01-C097111 and by the U.S. Army Research Office under Contract No. DAAH-04-96-0254.

[1] A. Ishimaru, *Wave Propagation and Scattering in Random Media*, IEEE/OUP Series on Electromagnetic Wave Theory (IEEE, Piscataway/Oxford University, Oxford, 1997), Chap. 7.
[2] D. S. Wiersma, P. Bartolini, A. Lagendijk, and R. Righini, Nature (London) **390**, 671 (1997).
[3] E. Akkermans, P. E. Wolf, R. Maynard, and G. Maret, J. Phys. (France) **49**, 77 (1988).
[4] J. W. Goodman, *Statistical Optics* (Wiley, New York, 1985), Chap. 5.
[5] B. G. Hoover, J. Opt. Soc. Am. A **16**, 1040 (1999).
[6] S. Feng, C. Kane, P. A. Lee, and A. D. Stone, Phys. Rev. Lett. **61**, 834 (1988).
[7] R. Berkovits, M. Kaveh, and S. Feng, Phys. Rev. B **40**, 737 (1989).
[8] D. Léger and J. C. Perrin, J. Opt. Soc. Am. **66**, 1210 (1976).
[9] A. Labeyrie, Astron. Astrophys. **6**, 85 (1970).
[10] T. R. Michel and K. A. O'Donnell, J. Opt. Soc. Am. A **9**, 1374 (1992).
[11] V. P. Ryabukho, V. L. Khomutov, O. P. Arshuk, A. A. Ghaussky, and I. F. Terent'eva, Proc. SPIE **2647**, 63 (1995).
[12] C. S. West and K. A. O'Donnell, Phys. Rev. B **59**, 2393 (1999).
[13] M. J. Rudd, J. Sci. Instrum. **2**, 55 (1969).
[14] A. Ishimaru, *Wave Propagation and Scattering in Random Media*, IEEE/OUP Series on Electromagnetic Wave Theory (IEEE Piscataway/Oxford University, Oxford, 1997), Chap. 14.
[15] A. Zardecki, S. A. W. Gerstl, W. G. Tani, and J. F. Embury, J. Opt. Soc. Am. A **3**, 393 (1986).
[16] F. Liu, K. M. Yoo, and R. R. Alfano, Opt. Lett. **19**, 740 (1994).
[17] A. Ishimaru, Y. Kuga, R. L.-T. Cheung, and K. Shimizu, J. Opt. Soc. Am. **73**, 131 (1983).
[18] T.-K. Chan, Y. Kuga, and A. Ishimaru, Waves Random Media **7**, 457 (1997).
[19] G. Zhang and L. Tsang, IEEE Trans. Geosci. Remote Sens. **36**, 1485 (1998).